Use of Spinel in Mineral Exploration: The Enigmatic Giant Mascot Ni-Cu-PGE Deposit – Possible Ties to Wrangellia and Metallogenic Significance

By Graham T. Nixon

KEYWORDS: Giant Mascot, spinel, chromite, indicator minerals, platinum-group elements, copper, nickel, magmatic sulphides, ultramafic rocks, metallogeny, Wrangellia.

INTRODUCTION

Numerous mineralogical and petrological studies over the last several decades have shown that spinel (chromite) is extremely sensitive to the ambient conditions of crystallization in magmatic environments and, as such, can be used as a petrogenetic indicator (Irvine, 1965, 1967). Whereas modern techniques in diamond exploration routinely rely on a suite of important indicator minerals (*e.g.* garnet, pyroxene, ilmenite), spinel is a sorely underutilized tool in the search for economic deposits of platinum-group elements (PGE) and Ni-Cu-PGE sulphides hosted by ultramafic and mafic rocks.

Spinel is present in most olivine-bearing ultramafic and gabbroic rocks where it generally forms a minor constituent (<2 vol. %), and although grains are usually small (commonly 5-20 µm, though some chromitites may contain grains reaching several millimetres), they are notably refractory and resistant to metamorphism and weathering. Previously, chromite grains in platinum nuggets recovered from placers along the Tulameen River were used to trace the origin of the PGE to chromitite horizons in the dunite core of the Tulameen Alaskan-type ultramafic complex (Nixon *et al.* 1990, 1997). In this paper, chromites occurring in ultramafic rocks which host the Giant Mascot Ni-Cu-PGE deposit are examined in order to identify their magmatic affinity and tectonic setting. This is made possible by the recently published global spinel database (Barnes and Roeder 2001; Roeder 1994) described briefly below.

THE TERRESTRIAL SPINEL DATABASE

The compilation of spinel compositions recently published by Barnes and Roeder (2001) is a comprehensive database of spinel analyses (>26 000) representing a wide variety of intrusive and extrusive mafic and ultramafic rocks formed in diverse tectonic settings. The extremely large volume of analytical data is subdivided into a number of categories and subcategories which include ophiolites, continental layered intrusions and flood basalts, island-arc tholeiites and oceanic basalts, boninites, alkalic and lamprophyric rocks, mantle xenoliths, Alaskan-type ultramafic intrusions and komatiites. Spinel populations in each category are represented by data density contour plots which allow for a quantitative comparison of spinels derived from different magma types and geological environments. The plots shown below are based on stoichiometrically-balanced spinel end-member components of the "spinel prism" (Stevens 1944) projected in ternary and binary diagrams.

GIANT MASCOT Ni-Cu-PGE DEPOSIT

The Giant Mascot Mine (1958-1974), the only past-producer of nickel in British Columbia, is situated about 20 kilometres north of Hope (Fig. 1). The mine produced a total of 4 191 035 tonnes of ore grading 0.77 % Ni and 0.34 % Cu along with minor cobalt, silver and gold, and an undetermined quantity of platinum-group elements. The Ni-Cu-PGE sulphide ores were mined from 22 distinct pipe-like to tabular ore shoots comprising heavily disseminated, semi-massive to massive sulphides hosted by peridotite and pyroxenite. The principal sulphide minerals are pyrrhotite, pentlandite, chalcopyrite and minor pyrite. The mineralogy, compositions and textures of the sulphides and coexisting ferromagnesian silicates are consistent with an orthomagmatic origin (Muir, 1971; McLeod, 1975). Further details of mine production, the mineral deposits and their host rocks are summarized by Pinsent (2002).

The geologic setting of the Giant Mascot ultramafic body is shown in Figure 1. The ultramafic rocks which host the sulphide ores are intruded and almost completely enveloped by the mid-Cretaceous Spuzzum Pluton, except to the east where the body is bounded by metasedimentary rocks (Settler schist). Contacts with the Spuzzum diorite are commonly marked by a narrow zone of hornblendite which appears to be a reaction phenomenon (Aho, 1956). Details of the geology together with excellent reviews of previous work in the area are given by Ash (2002) and Pinsent (2002).

Despite recent advances in our understanding of the regional geology (Ash 2002) and geochemistry of the rocks which host the Cu-Ni-PGE deposits (Pinsent 2002), the petrotectonic setting of Giant Mascot remains enigmatic. For example, the nature of the contact between the ultramafic body and Spuzzum diorite has been debated (*e.g.*
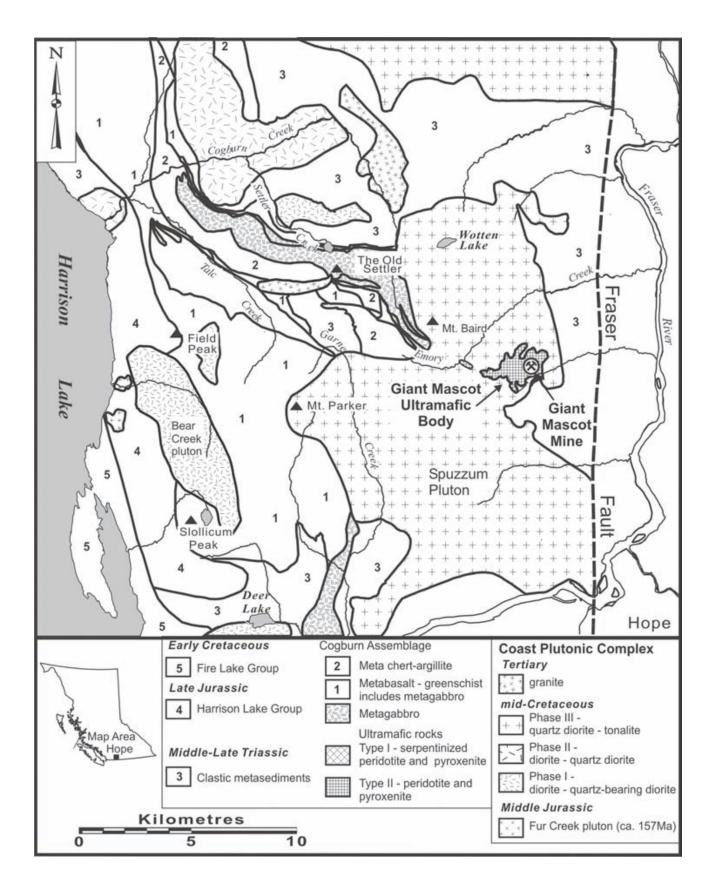
Figure 1. Location and geologic setting of the former Giant Mascot Ni-Cu-PGE mine, southern British Columbia (after Ash, 2002).

Cockfield and Walker, 1933; Aho, 1956; McLeod *et al.,* 1976); and the ultramafic rocks were once considered to be an early differentiate of the calc-alkaline Spuzzum Pluton (*e.g.* McLeod *et al.*, 1976). This conclusion appears difficult to reconcile with the common association of Ni-Cu-PGE sulphide ores with tholeiitic magmatic environments (*e.g.* Hulbert, 2001). The most recent geological investigations have concluded that the Giant Mascot ultramafic body is intruded by, and therefore older than, Spuzzum diorite, and represents either a partially engulfed ophiolite fragment analogous to those farther west in the Cogburn Assemblage (Ash, 2002; Fig. 3); or serves as a host to "gabbro-related" magmatic sulphide ores of unknown age and origin (Pinsent 2002).

PETROTECTONIC SETTING OF GIANT MASCOT

SPINEL DATA

The composition of chrome spinels occurring in ultramafic rocks and ores at Giant Mascot provide information that is directly relevant to the origin of the ultramafic body and thus independent of interpretations regarding external geological relationships.

In his study of the 4600 Level ore body, Muir (1971) made a number of electron-microprobe analyses of spinel grains in both ore-bearing and barren pyroxenites and peridotites, including olivine- and clinopyroxene-bearing hornblende orthopyroxenites and hornblende harzburgites and their sulphide-rich equivalents. The amount of amphibole in these rocks appears unique to the 4600 Level orebody when compared to the more olivine-enriched ores described by Aho (1956). The mineralized samples contain variable proportions of ferromagnesian silicates and Fe-Ni and Cu sulphides, and ores typically exhibit semi-massive to blebby to net-textured sulphides. The analyzed spinels include euhedral grains in unaltered olivine and orthopyroxene as well as a random sampling of grains whose host mineral is not specified. The quality of the electron-probe analyses is difficult to assess: some minor elements were not determined (Mn, Zn and V); oxide totals are generally high (range = 98.3-104.2 wt %; arithmetic mean = 101.3 wt %) but vary slightly depending on the details of the Fe_2O_3 recalculation procedure; at the very least, the analyses do appear to be consistent with spinel stoichiometry.

SPINEL PLOTS

The compositions of Giant Mascot (GM) spinels are shown below in three diagrams based on standard projections of the spinel prism: a triangular Cr-Al-Fe^{3+} plot representing projection onto the face of the prism and cation ratio plots of Cr/(Cr+Al) (or Cr#) and $Fe^{3+}/(Cr+Al+Fe^{3+})$ (or Fe3#) *vs* $Fe^{2+}/(Mg+Fe^{2+})$ (or Fe2#); and a fourth plot of TiO_2 vs $Fe^{2+}/(Mg+Fe^{2+})$ (Ti plot). Data density contours for selected categories or subcategories of spinel compositions in the global database are also shown at the 50th and 90th percentiles (*i.e.* 50% and 90%, respectively, of analyses in

the category/subcategory of the database fall within these contours).

Figure 2 compares GM spinels with the composition of spinels in metamorphic terranes at greenschist, amphibolite and higher grades of metamorphism. From details of compositional zoning given by Muir (1971), it is clear that some GM spinel grains support rims and/or areas of secondary magnetite and "ferritchromit" that fall at the Fe3+ apex or close to the Cr-Fe3+ join, respectively, in the triangular plot, and have similar compositions to metamorphic spinels (Fig. 2d provides the best discriminant).

Spinels that last equilibrated with Fe-Ni sulphides are compared to GM spinel compositions in Figure 3. The latter are clearly displaced from the global array in the tiangular and Cr# plots, and very few GM spinel grains appear to have equilibrated with magmatic sulphide. Clearly, the overall curvilinear trends of GM spinels in these plots appear consistent with trends formed at high temperatures during crystal-liquid equilibration and subsolidus exchange reactions between spinel and its host silicate phase. It is valid, therefore, to compare the trends of GM spinels with those in the global database to derive information regarding their igneous affiliation.

Figures 4-6 show the compositional fields for spinels derived from ultramafic-mafic rocks in selected oceanic environments and include ocean floor (abyssal) peridotites, ophiolites (including tectonized peridotites and ultramafic-mafic cumulates), and high-pressure, high-temperature "Alpine" peridotites. Relative to oceanic rocks, GM spinels contain significantly higher Fe^{+3}, and in the Cr# and Fe3# plots spinel compositions are displaced to higher Fe^{2+}.

Figure 7 examines potential relationships with Alaskan-type ultramafic intrusions. Although the Ti plot shows a reasonable correspondence with GM spinels, the latter trend is displaced towards higher Fe2# on the Cr# and Fe3# plots. In addition, the triangular plot shows a clear distinction between GM and Alaskan-type spinels which lie closer to the Cr-Fe^{3+} join. This observation is also supported by the presence of cumulus orthopyroxene at Giant Mascot since this phase is typically absent in Alaskan-type ultramafic complexes.

Comparisons with spinels from layered intrusions are shown in Figure 8. All of these plots (Fig. 8a-d) show a close overall correspondence between spinels from layered intrusions and the GM spinel trend. Small aberrations are apparent in the Cr# plot where three GM spinel analyses fall outside the 90th percentile contour (Fig. 8c), and on the Ti plot where a cluster of spinel analyses fall within a population density minimum (Fig. 8b).

The fields for subvolcanic intrusions in flood basalt provinces are shown in Figure 9. As with layered intrusions, there is good overall agreement between the GM spinel trend and the global array. The population density minimum in the Ti plot is no longer evident although there is a slightly greater discrepancy in the Cr# plot for low Cr# GM spinels. This category of spinels, and those from layered intrusions, represent the closest analogues to the compositions of GM spinels.
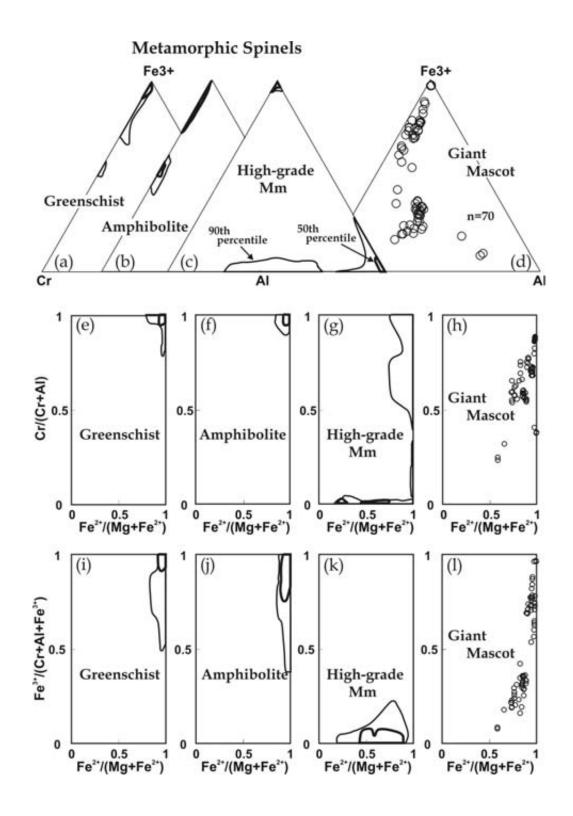
Figure 2. Trivalent cation, $Cr/(Cr+Al)$ vs $Fe^{2+}/(Mg+Fe^{2+})$ and $Fe^{3+}/(Cr+Al+Fe^{3+})$ vs $Fe^{2+}/(Mg+Fe^{2+})$ plots for spinel compositions in greenschist (a, e, i), amphibolite(b, f, j) and high-grade metamorphic rocks (c, g, k) from various protoliths (including komatiites) compared to spinels from Giant Mascot (d, h, i). The field outlines represent contours of the density of spinel populations for the subcategory in the global database of Barnes and Roeder (2001) given at the 50th and 90th percentiles (i.e. 50% and 90% of analyses in the subcategory fall within the 50th (thick line) and 90th (thin line) percentile contours, respectively). Note that the curvilinear trends of Giant Mascot spinel analyses taken from Muir (1971) are readily distinguished from spinel compositions at each grade of metamorphism when all three plots are taken into account.
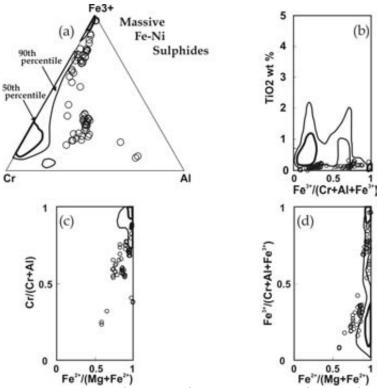
Figure 3. Plots of (a) trivalent cations, (b) TiO_2 vs $Fe^{3+}/(Cr+Al+Fe^{3+})$, (c) $Cr/(Cr+Al)$ vs $Fe^{2+}/(Mg+Fe^{2+})$ and (d) $Fe^{3+}/(Cr+Al+Fe^{3+})$ vs $Fe^{2+}/(Mg+Fe^{2+})$ for Giant Mascot spinels showing data density contours (as in Fig. 2) for spinels at the margins of massive Fe-Ni ore bodies taken from the global database. The lack of equilibration between Giant Mascot spinels and sulphides is clearly evident in plots (a) and (c).
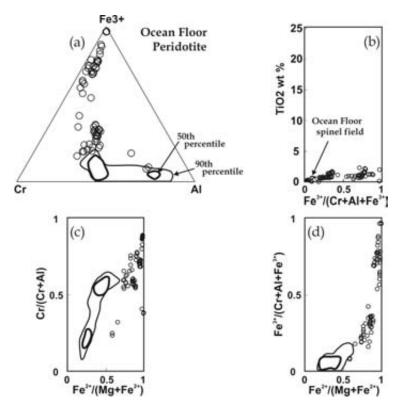

Figure 4. Plots of (a) trivalent cations, (b) TiO_2 vs $Fe^{3+}/(Cr+Al+Fe^{3+})$, (c) $Cr/(Cr+Al)$ vs $Fe^{2+}/(Mg+Fe^{2+})$ and (d) $Fe^{3+}/(Cr+Al+Fe^{3+})$ vs $Fe^{2+}/(Mg+Fe^{2+})$ for Giant Mascot spinels showing data density contours for spinels from ocean floor (abyssal) peridotites. Note the overall higher Fe^{3+} and TiO_2 contents, and higher $Fe/(Mg+Fe)$ ratios of Giant Mascot spinels.
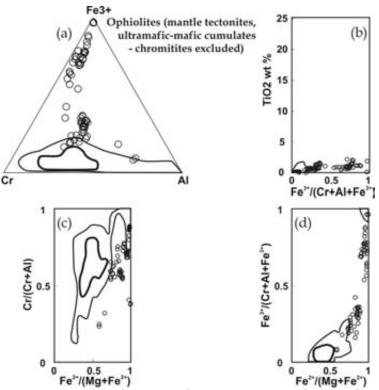
Figure 5. Plots of (a) trivalent cations, (b) TiO_2 *vs* $Fe^{3+}/(Cr+Al+Fe^{3+})$, (c) $Cr/(Cr+Al)$ *vs* $Fe^{2+}/(Mg+Fe^{2+})$ and (d) $Fe^{3+}/(Cr+Al+Fe^{3+})$ *vs* $Fe^{2+}/(Mg+Fe^{2+})$ for Giant Mascot spinels showing data density contours for spinels from ophiolite complexes including tectonized ultramafic rocks and ultramafic-mafic cumulates (chromitite seams excluded). Note that Giant Mascot spinels generally have higher Fe^{3+} contents and $Fe/(Mg+Fe)$ at equivalent $Cr/(Cr+Al)$ ratios.
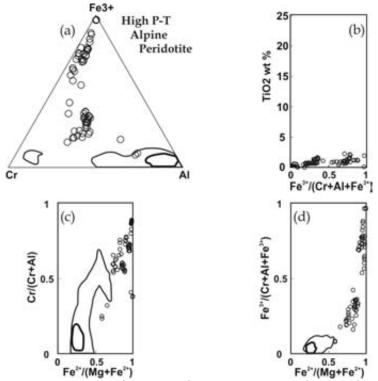

Figure 6. Plots of (a) trivalent cations, (b) TiO_2 *vs* $Fe^{3+}/(Cr+Al+Fe^{3+})$, (c) $Cr/(Cr+Al)$ *vs* $Fe^{2+}/(Mg+Fe^{2+})$ and (d) $Fe^{3+}/(Cr+Al+Fe^{3+})$ *vs* $Fe^{2+}/(Mg+Fe^{2+})$ for Giant Mascot spinels showing data density contours for spinels from tectonically emplaced, high-pressure, high-temperature "Alpine" ultramafic bodies of probable ophiolitic affinity in orogenic belts. Note the overall higher Fe^{3+} contents and $Fe/(Mg+Fe)$ ratios of Giant Mascot spinels.
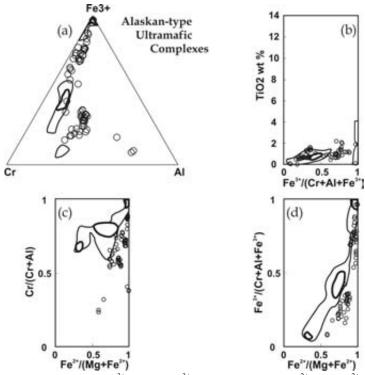
Figure 7. Plots of (a) trivalent cations, (b) TiO_2 vs $Fe^{3+}/(Cr+Al+Fe^{3+})$, (c) $Cr/(Cr+Al)$ vs $Fe^{2+}/(Mg+Fe^{2+})$ and (d) $Fe^{3+}/(Cr+Al+Fe^{3+})$ vs $Fe^{2+}/(Mg+Fe^{2+})$ for Giant Mascot spinels showing data density contours for spinels from Alaskan-type ultramafic complexes. Note that Giant Mascot spinel trends are slightly but systematically displaced to higher Fe/(Mg+Fe) in plots (c) and (d); and are best distinguished from Alaskan-type complexes on the Cr-Al-Fe^{3+} plot.
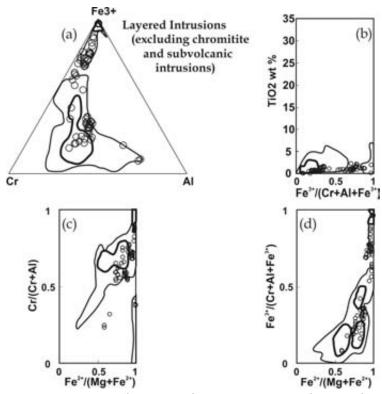

Figure 8. Plots of (a) trivalent cations, (b) TiO_2 vs $Fe^{3+}/(Cr+Al+Fe^{3+})$, (c) $Cr/(Cr+Al)$ vs $Fe^{2+}/(Mg+Fe^{2+})$ and (d) $Fe^{3+}/(Cr+Al+Fe^{3+})$ vs $Fe^{2+}/(Mg+Fe^{2+})$ for Giant Mascot spinels showing data density contours for spinels from layered continental mafic-ultramafic intrusions (excluding chromitite seams and subvolcanic intrusion subcategories). Note the close correspondence between layered intrusion and Giant Mascot spinel trends.
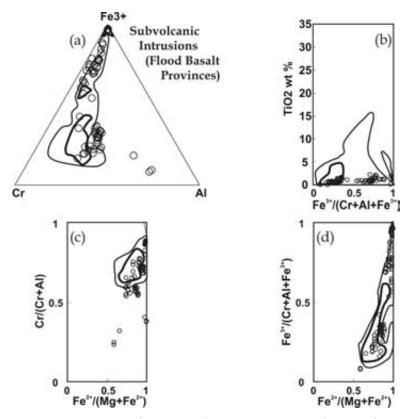
Figure 9. Plots of (a) trivalent cations, (b) TiO_2 vs $Fe^{3+}/(Cr+Al+Fe^{3+})$, (c) $Cr/(Cr+Al)$ vs $Fe^{2+}/(Mg+Fe^{2+})$ and (d) $Fe^{3+}/(Cr+Al+Fe^{3+})$ vs $Fe^{2+}/(Mg+Fe^{2+})$ for Giant Mascot spinels showing data density contours for spinels from continental mafic-ultramafic subvolcanic intrusions in flood basalt provinces. As in Fig. 8, note the close correspondence between subvolcanic intrusion and Giant Mascot spinel trends.

SIGNIFICANCE OF SPINEL DATA

Comparisons of the composition of GM spinels with the global spinel database indicate that the ultramafic rocks which host the Ni-Cu-PGE deposits are not derived from an obducted oceanic terrane, nor are they related to Alas-kan-type ultramafic intrusions such as the Tulameen complex. Instead, the spinels at Giant Mascot exhibit a strong affinity with the major continental layered intrusions and smaller subvolcanic intrusions in flood basalt provinces, both of which have a tholeiitic magmatic association. The only igneous province in the northern Cordillera currently recognized to contain a component of tholeiitic flood basalt volcanism, the Late Triassic Karmutsen-Nicolai province, is Wrangellia. This correlation also satisfies the most recent interpretations that the Giant Mascot ultramafic body is in-truded by mid-Cretaceous plutonic rocks. According to the compositions of chrome spinels in host rocks and ores, therefore, the Giant Mascot ultramafic body represents a high-level intrusive fragment of the Late Triassic accreted terrane of Wrangellia accidently incorporated in the Spuzzum Pluton. This conclusion may be tested geologi-cally, and, if correct, has important tectonic and metallo-genic ramifications as discussed below.

TECTONIC IMPLICATIONS

The boundaries of Wrangellia in the southern Coast Belt are not well known at present (Fig. 10). Currently de-fined limits are based on vestiges of distinctive Wrangellian stratigraphy, as typified by Late Triassic Quatsino lime-stone and Karmutsen basalts (Jones *et al*. 1977), which are found as scattered pendants and septa of marble and greenschist to amphibolite-grade metabasalts in Middle to Late Jurassic and Cretaceous granitoid rocks of the Coast Plutonic Complex. The southern margin of Wrangellia ap-pears to be buried by northwesterly verging, early Late Cre-taceous structures of the San Juan – Cascade thrust system (Brandon *et al*., 1988), and by structurally stacked oceanic basin and arc terranes in the southeastern Coast Mountains (*i.e.* east of Harrison Lake; and *see* Ash (2002) for a differ-ent structural interpretation of surface exposures in this re-gion). Based on seismic refraction and reflection profiles, Wrangellia appears to form much of the lower and middle crust of the southwestern Coast Belt, and may extend into the 30 km-thick, complexly deformed crust of the south-eastern Coast Belt (Zelt *et al*., 1993; Monger and Journeay, 1994). These arguments have been used to infer the south-ern limit of Wrangellia in the subsurface shown in Figure 10. Note that this inferred boundary is essentially coinci-dent with the location of Giant Mascot. Thus, the interpre-tation of the spinel data offered above is consistent with the inferred continuation of Wrangellia to the east where it is
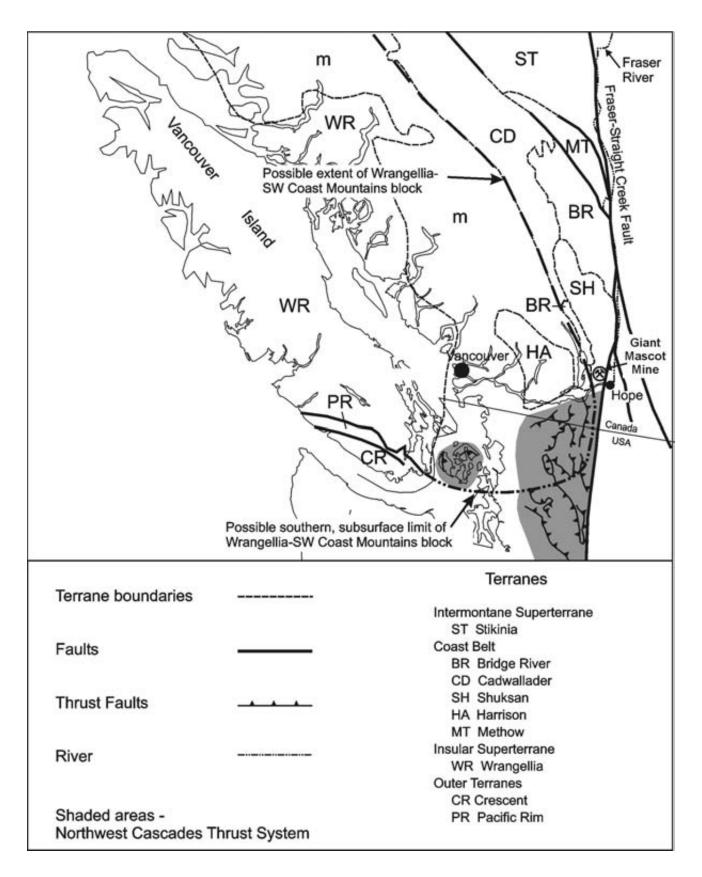
Figure 10. Terrane assemblage map of the southern Coast Belt showing the location of the Giant Mascot ultramafic body in relation to known and inferred boundaries for Wrangellia (modified from Monger and Journeay, 1994).
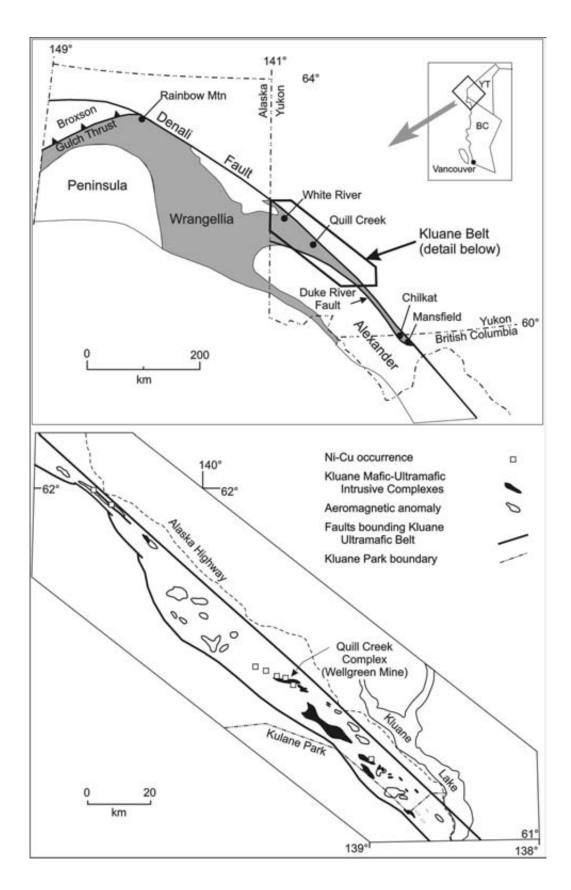
Figure 11. Generalized tectonic setting of the Kluane ultramafic belt in the Yukon showing the location of ultramafic-mafic intrusive complexes at the eastern margin of the Wrangellia accreted terrane and their associated Ni-Cu-PGE deposits (after Hulbert, 1997).

probably truncated by the Fraser - Straight Creek fault system.

METALLOGENIC SIGNIFICANCE

Mafic-ultramafic intrusions that host magmatic Ni-Cu-PGE sulphide deposits and prospects are known in northern Wrangellia along the Denali (Shakwak) fault system in Alaska and the Yukon Territory (Fig. 11). The Kluane mafic-ultramafic belt contains the largest known concentration of these intrusions and their mineral deposits, and coincidently(?), occupies a setting analogous to Giant Mascot at the eastern margin of Wrangellia. The southern extension of this belt crosses into northernmost British Columbia in the form of the Chilkat and Mansfield complexes (Fig. 11). The largest mafic-ultramafic bodies form sill-like subvolcanic intrusions (≤600m thick) preferentially emplaced in pyritic metasedimentary strata of Pennsylvanian-Permian age and comagmatic with Middle(?) to Late Triassic Nicolai volcanic rocks (Hulbert 1997). One of the largest intrusions in the Kluane belt, the Quill Creek complex, hosts the former Wellgreen mine, the only past-producer of Ni-Cu ore in the Yukon. Of the initial reserves of 669 150 tonnes of ore, only 171 652 tonnes were mined (1972-73) with an average grade of 2.23% Ni, 1.39% Cu, 0.073% Co and 2.15 ppm Pt and Pd (Hulbert 1997). The sulphide ores have similar mineralogy (pyrrhotite-pentlandite-chalcopyrite-pyrite) and textures

(massive, semi-massive and disseminated sulphides) to those at Giant Mascot, and with respect to the PGE, over 20 species of platinum-group minerals have been identified (Barkov *et al.*, 2002). Further details of the Kluane intrusions and their mineral deposits may be found in Hulbert (1997).

The similarities noted above between the petrotectonic setting and nature of Ni-Cu-PGE deposits in mafic-ultramafic rocks of the Kluane belt and Giant Mascot also extend to their spinel compositions. Chromites in Kluane ultramafic-mafic intrusions are compared with the global data array for layered intrusions and subvolcanic intrusions in flood basalt provinces in Figures 12 and 13, respectively. In all these plots, Kluane spinels are coincident with the global data density maxima for spinels from continental tholeiitic intrusions. The compositions of spinels from Giant Mascot are plotted with Kluane spinels in Figure 14. Note the similarity of Kluane and GM spinel compositions at the Fe^{3+}-poor end of the spinel populations, and the more extensive Fe^{3+}-enrichment of GM spinels (Figs. 14a and b). The divergence in Kluane and GM spinel trends in the Ti plot (Fig. 14b) may be a function of different crystal-liquid fractionation histories or reflect variable TiO_2 contents of parental magmas in the Kluane belt. Notwithstanding these details, the overall similarity of spinel compositions in ultramafic rocks at Kluane and Giant Mascot is striking and strengthens arguments advanced above for a similar petrotectonic and metallogenic setting.
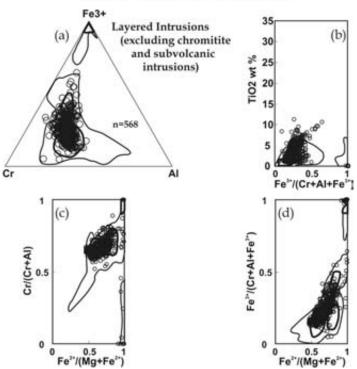

Figure 12. Plots of (a) trivalent cations, (b) TiO_2 *vs* $Fe^{3+}/(Cr+Al+Fe^{3+})$, (c) $Cr/(Cr+Al)$ *vs* $Fe^{2+}/(Mg+Fe^{2+})$ and (d) $Fe^{3+}/(Cr+Al+Fe^{3+})$ *vs* $Fe^{2+}/(Mg+Fe^{2+})$ for spinels from mafic-ultramafic intrusions at the eastern margin of Wrangellia in the Yukon and Alaska (spinel data from Hulbert, personal communication, 2002; and *see* Hulbert 1997). Data density contours are for spinels in layered intrusions (Fig. 8). Note the correspondence of data density maxima in all plots.
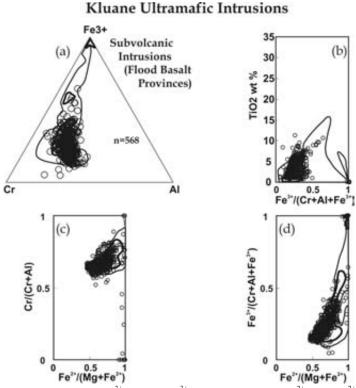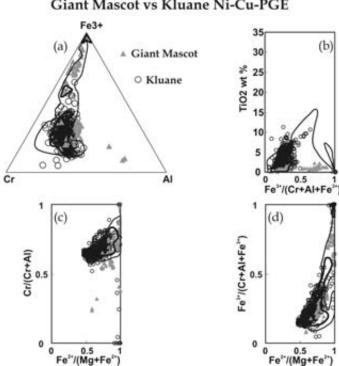
Kluane Ultramafic Intrusions

Figure 13. Plots of (a) trivalent cations, (b) TiO_2 vs $Fe^{3+}/(Cr+Al+Fe^{3+})$, (c) $Cr/(Cr+Al)$ vs $Fe^{2+}/(Mg+Fe^{2+})$ and (d) $Fe^{3+}/(Cr+Al+Fe^{3+})$ vs $Fe^{2+}/(Mg+Fe^{2+})$ for Giant Mascot spinels showing data density contours for spinels from continental mafic-ultramafic subvolcanic intrusions in flood basalt provinces. As in Fig. 12, note the correspondence of data density maxima in all plots.

Giant Mascot vs Kluane Ni-Cu-PGE

Figure 14. Plots of (a) trivalent cations, (b) TiO_2 vs $Fe^{3+}/(Cr+Al+Fe^{3+})$, (c) $Cr/(Cr+Al)$ vs $Fe^{2+}/(Mg+Fe^{2+})$ and (d) $Fe^{3+}/(Cr+Al+Fe^{3+})$ vs $Fe^{2+}/(Mg+Fe^{2+})$ for Giant Mascot and Kluane spinels showing data density contours for spinels from subvolcanic intrusions in flood basalt provinces. Note the close correspondence between the datasets and the more extensive Fe-enrichment of Giant Mascot spinels along the global data array.

Based on these spinel compositions, therefore, the mineral deposit model that most closely approximates Giant Mascot appears to be the world-class Noril'sk-Talnakh Ni-Cu-PGE ores which are hosted by subvolcanic intrusions associated with the Triassic Siberian flood basalt province (deposit type 5b of Cox and Singer, 1986). Differences between this deposit type and Giant Mascot include the fact that the latter ores are hosted by ultramafic rocks, and these lithologies carry igneous amphibole as an important constituent. The gabbroid-associated Ni-Cu-PGE deposit type favoured for Giant Mascot by Eckstrand (1984, deposit type 12.2.c for stock-like intrusions) seems inappropriate because these deposits are considered to be associated with orogenic as opposed to extensional or plume-related tectonic settings.

CONCLUDING REMARKS

It has been shown above that spinels can be usefully employed as "indicator minerals" in the search for economically attractive ultramafic-mafic-hosted Ni-Cu-PGE deposits in the Cordillera. In the case of Giant Mascot, the available spinel data provide new insight into the petrotectonic setting and metallogenic significance of this seemingly unusual deposit type. Spinel compositions indicate that the Giant Mascot ultramafic body and its associated ore deposits represent a fragment of the Late Triassic Wrangellian flood basalt province. Furthermore, the Ni-Cu-PGE sulphide ores at Giant Mascot are not unique but related to similar deposits described in Alaska and the Yukon which share the same tectonic setting and mineral deposit type. If correct, this interpretation presents new opportunities for base and precious metal mineral exploration in the southern Insular Belt, particularly along the poorly defined eastern margin of Wrangellia where most documented occurrences in the northern Cordillera are concentrated.

As a caveat, it must be emphasized that: 1) these conclusions are based on a single set of electron-microprobe analyses made by Muir (1971) over 30 years ago; and 2) the analyzed chromites represent samples collected from ultramafic rocks associated with just one (4600 Level) of at least 28 different ore shoots. A more comprehensive suite of samples is currently being analyzed in order to check the spinel compositions on which this paper is based in an attempt to corroborate these conclusions.

ACKNOWLEDGMENTS

Thanks are extended to Kirk Hancock for drafting some of the figures. Any errors or omissions are the sole responsibility of the author.

REFERENCES

Aho, A. E. (1956): Geology and genesis of ultrabasic nickel-copper-pyrrhotite deposits at the Pacific Nickel property, southwestern British Columbia; *Economic Geology*, Volume 51, pages 444-481.

Ash, C. H. (2002): Geology of the East Harrison Lake Belt, southwestern British Columbia; *in* Geological Fieldwork 2001, *British Columbia Ministry of Energy and Mines*, Paper 2002-1, pages 197-210.

Barkov, A. Y., Laflamme, J. H. G., Cabri, L. J. and Martin, R. F. (2002): Platinum-group minerals from the Wellgreen Ni-Cu-PGE deposit, Yukon, Canada; *Canadian Mineralogist*, Volume 40, pages 651-669.

Barnes, S. J. and Roeder, P. L. (2001): The range of spinel compositions in terrestrial mafic and ultramafic rocks; *Journal of Petrology*, Volume 42, pages 2279-2302.

Brandon, M. T., Cowan, D. S. and Vance, J. A. (1988): The Late Cretaceous San Juan thrust system, San Juan Islands; *Geological Society of America*, Special Paper 221, 81 pages.

Cockfield, W. E. and Walker, J. F. (1933): The nickel-bearing rocks near Choate, British Columbia; *Geological Survey of Canada*, Summary Report 1933, Part A, pages 62-68.

Cox, D. P. and Singer, D. A., Editors (1986): Mineral deposit models; *United States Geological Survey*, Bulletin 1693, 379 pages.

Eckstrand, O. R., Editor (1984): Canadian mineral deposit types: a geological synopsis; *Geological Survey of Canada,* Economic Geology Report 36, 86 pages.

Hulbert, L. J. (1997): Geology and metallogeny of the Kluane mafic-ultramafic belt Yukon Territory, Canada: eastern Wrangellia – a new Ni-Cu-PGE metallogenic terrane; *Geological Survey of Canada*, Bulletin 506, 265 pages.

Hulbert, L. J. (2001): GIS maps and databases of mafic-ultramafic hosted Ni, Cu-Ni, Cr ± PGE occurrences and mafic-ultramafic bodies in British Columbia; *British Columbia Ministry of Energy and Mines*, Geoscience Map 2001-2.

Irvine, T. N. (1965): Chromium spinel as a petrogenetic indicator. Part 1. Theory; *Canadian Journal of Earth Sciences*, Volume 2, pages 648-672.

Irvine, T. N. (1967): Chromium spinel as a petrogenetic indicator. Part 2. Petrologic applications; *Canadian Journal of Earth Sciences*, Volume 4, pages 71-103.

Jones, D. L., Silberling, N. J. and Hillhouse, J. (1977): Wrangellia: a displaced terrane in northwestern North America; *Canadian Journal of Earth Sciences*, Volume 14, pages 2565-2577.

McLeod, J. A. (1975): The Giant Mascot ultramafite and its related ores; unpublished M.Sc. thesis, *The University of British Columbia,* 123 pages.

McLeod, J. A., Vining, M. and McTaggart, K. C. (1976): Note on the age of the Giant Mascot ultramafic body, near Hope, B.C.; *Canadian Journal of Earth Sciences*, Volume 13, pages 1152-1154.

Monger, J. W. H. and Journeay, J. M. (1994): Basement geology and tectonic evolution of the Vancouver region; *in* Geology and Geologic Hazards of the Vancouver Region, southwestern British Columbia, J. W. H. Monger (editor), *Geological Survey of Canada*, Bulletin 481, pages 3-25.

Muir, J. E. (1971): A study of the petrology and ore genesis of the Giant Nickel 4600 ore body, Hope, British Columbia; unpublished M.Sc. Thesis, *The University of Toronto*, 125 pages.

Nixon, G. T., Cabri, L. J. and Laflamme, J. H. G. (1990): Platinum-group-element mineralization in lode and placer deposits associated with the Tulameen Alaskan-type Complex, British Columbia; *Canadian Mineralogist*, Volume 28, p. 503-535.

Nixon, G. T., Hammack, J. L., Ash, C. H., Cabri, L. J., Case, G., Connelly, J. N., Heaman, L. M., Laflamme, J. H. G., Nuttall, C., Paterson, W. P. E. and Wong, R. H. (1997): Geology and platinum-group-element mineralization of Alaskan-type ultramafic-mafic complexes in British Columbia; *British*

Columbia Ministry of Employment and Investment, Bulletin 93, 141 pages.

Pinsent, R. H. (2002): Ni-Cu-PGE potential of the Giant Mascot and Cogburn ultramafic-mafic bodies, Harrison-Hope area, southwestern British Columbia (092H); *in* Geological Field-work 2001, *British Columbia Ministry of Energy and Mines*, Paper 2002-1, pages 211-236.

Roeder, P. L. (1994): Chromite: from the fiery rain of chondrules to the Kilauea Iki lava lake; *Canadian Mineralogist*, Volume 32, pages 729-746.

Stevens, R. E. (1944): Compositions of some chromites of the western hemisphere; *American Mineralogist*, Volume 29, pages 1-34.

Zelt, B. C., Ellis, R. M. and Clowes, R. M. (1993): Crustal velocity structure in the eastern Insular and southernmost Coast belts, Canadian Cordillera; *Canadian Journal of Earth Sciences*, Volume 30, pages 1014-1027.